J Cachexia Sarcopenia Muscle
DOI 10.1007/s13539-012-0062-x

ORIGINAL ARTICLE

Inflammation, organomegaly, and muscle wasting despite hyperphagia in a mouse model of burn cachexia

Felipe E. Pedroso · Paul B. Spalding · Michael C. Cheung · Relin Yang · Juan C. Gutierrez · Andrea Bonetto · Rui Zhan · Ho Lam Chan · Nicholas Namias · Leonidas G. Koniaris · Teresa A. Zimmers

Received: 1 December 2011 / Accepted: 15 February 2012

Abstract
Background Burn injury results in a chronic inflammatory, hypermetabolic, and hypercatabolic state persisting long after initial injury and wound healing. Burn survivors experience a profound and prolonged loss of lean body mass, fat mass, and bone mineral density, associated with significant morbidity and reduced quality of life. Understanding the mechanisms responsible is essential for developing therapies. A complete characterization of the pathophysiology of burn cachexia in a reproducible mouse model was lacking.
Methods Young adult (12–16 weeks of age) male C57BL/6J mice were given full thickness burns using heated brass plates or sham injury. Food and water intake, organ and muscle weights, and muscle fiber diameters were measured. Body composition was determined by Piximus. Plasma analyte levels were determined by bead array assay.
Results Survival and weight loss were dependent upon burn size. The body weight nadir in burned mice was 14 days, at which time we observed reductions in total body mass, lean carcass mass, individual muscle weights, and muscle fiber cross-sectional area. Muscle loss was associated with increased expression of the muscle ubiquitin ligase, MuRF1. Burned mice also exhibited reduced fat mass and bone mineral density, concomitant with increased liver, spleen, and heart mass. Recovery of initial body weight occurred at 35 days; however, burned mice exhibited hyperphagia and polydipsia out to 80 days. Burned mice had significant increases in serum cytokine, chemokine, and acute phase proteins, consistent with findings in human burn subjects.
Conclusions This study describes a mouse model that largely mimics human pathophysiology following severe burn injury. These baseline data provide a framework for mouse-based

Felipe E. Pedroso, Paul B. Spalding, and Michael C. Cheung contributed equally to this work.

F. E. Pedroso · A. Bonetto · T. A. Zimmers (✉)
Department of Cancer Biology, Kimmel Cancer Center,
Thomas Jefferson University,
233 South 10th. Street BLSB 306,
Philadelphia, PA 19107, USA
e-mail: tzimmers@kimmelcancercenter.org

P. B. Spalding · M. C. Cheung · R. Yang · J. C. Gutierrez · H. L. Chan · N. Namias · T. A. Zimmers
DeWitt Daughtry Family Department of Surgery,
University of Miami Miller School of Medicine,
Miami, FL, USA

P. B. Spalding · N. Namias · T. A. Zimmers
Division of Burns,
University of Miami Miller School of Medicine,
Miami, FL, USA

R. Zhan · T. A. Zimmers
Graduate Program in Cancer Biology, Sylvester Comprehensive Cancer Center, University of Miami Miller School of Medicine,
Miami, FL, USA

L. G. Koniaris · T. A. Zimmers
Department of Surgery, Thomas Jefferson University,
Philadelphia, PA, USA

T. A. Zimmers
Department of Surgery, Kimmel Cancer Center, Thomas Jefferson University,
233 South 10th. Street BLSB 306,
Philadelphia, PA 19107, USA

Published online: 29 March 2012

pharmacological and genetic investigation of burn-injury-associated cachexia.

Keywords Thermal injury · Muscle wasting · Muscle atrophy · Metabolism · Animal model

1 Introduction

According to statistics provided by the American Burn Association [1], there are 450,000 burns annually in the USA, of which 3,500 result in death. There are 45,000 hospitalizations for burn injury, with 31% of burns exceeding 10% total body surface area (TBSA) and 11% exceeding 20% TBSA [2]. Worldwide, burn injuries are on the rise due to increased industrialization, escalating conflicts and the use of white phosphorus on battlefields. Fortunately, advances in burn care are resulting in greater survival for patients with severe burns; however, this increases the need for long-term care of these challenging patients through the acute post-burn period into the convalescent period [3, 4].

Morbidity and mortality are associated with burn size [1]. Severe burn injuries are associated with a significant inflammatory, hypermetabolic (increased body temperature, oxygen and glucose consumption, and CO_2 production), and hypercatabolic (increased lipolysis, proteolysis, glycogenolysis) state, with hepatosplenomegaly that arises acutely and persists chronically. Studies have shown that this profound and prolonged hypermetabolic and hyperinflammatory state persist for up to 3 years after initial burn injury and even following wound healing [3–5]. Consequently, patients develop a systemic loss of muscle mass, lean body mass, and bone mineral density [3–6]. Patients with a 40% TBSA burn can lose up to 25% of their total body mass in 3–4 weeks, with generally fatal consequences [5, 7]. Lesser weight loss of even 10–15%, however, is associated with significantly increased rates of infection and reduced wound healing. Such persistent inflammation and cachexia is common in all trauma, surgical and critically ill patients, and many forms of chronic diseases, but the severity and chronicity in burn patients is unique [8]. In all cases, weight loss and the rate of weight loss are closely correlated with mortality [9].

The metabolic response to burn injury is characterized by changes in protein metabolism occurring in multiple organs and tissues. The breakdown of skeletal muscle, the largest protein and amino acid stores in the body, through increased proteolysis, leads to negative nitrogen balance and whole-body protein loss [5, 10, 11]. Muscle wasting is exacerbated by insulin and insulin-like growth factor resistance leading to reduced anabolism [12]. The imbalance in anabolic and catabolic pathways leads to muscle atrophy, weakness, and debilitation. In contrast, protein synthesis and anabolic pathways are increased in the liver and intestinal mucosa. Indeed, hepatomegaly and splenomegaly are frequently observed and are likely in large part due to induction of the acute phase response and increased hepatic protein synthetic capacity [13, 14].

Although investigators have used mouse models to dissect molecular pathways altered after burn injury [15–18], to date no single study has measured the long-term effects of burn injury on body weight, muscle weight, fat weight, bone mass, and food and water intake in a mouse model. This basic information is necessary to provide a framework and baseline for evaluating the mechanisms underlying burn-injury-associated cachexia. Moreover, although the burn response in humans scales with percentage of body surface burned, most reported murine models employ fixed templates for scald or flame injury, an approach that does not permit fine adaptation of the burn area for mice of differing sizes and shapes. Finally, although heightened food intake has been reported in rats after burn injury, an absence of publications on the murine response has led to referees asking for pair-fed models. Taken together the absence of muscle-specific data, the variation inherent in existing models, and confusion in the field regarding food intake, we sought to develop a robust, reproducible, well-documented model of burn-injury-associated cachexia in mice.

In this model, similar to human burn patients, mice show reduced total body weight, fat, and lean body mass persisting long after initial injury and wound healing. We also observed loss of bone mineral density, hepatosplenomegaly and cardiac hypertrophy. Using samples from mice at the nadir of body weight, we also measure muscle fiber morphometry, cytokine/chemokine/acute phase protein levels, and muscle gene expression. We anticipate these data will prove useful for further analysis of pathways mediating burn-injury-associated cachexia and likely other metabolic sequelae.

2 Methods

2.1 Mice

All experiments were approved by the University of Miami and Thomas Jefferson University Institutional Animal Care and Use Committees. Mice were cared for in accordance with the National Research Council's Guide for the Care and Use of Laboratory Animals. Male C57BL/6J mice (Jackson Laboratory, Bar Harbor, ME, USA) 12–16 weeks old were acclimated to the colony for at least 1 week prior to injury with free access to standard chow and water and a 12-h light–dark cycle in standard acrylic cages with paper or wood chip bedding. While mice were specific pathogen free or virus antibody free at time of purchase, the mice described were housed in a conventional facility without

barrier housing, autoclaving, sterile cages, or negative pressure. Mice were housed four per cage until the day of injury in acrylic cages with wire tops and plastic filter lids. Mice were fed certified rodent diet LabDiet 5002 (Purina), with 20% protein, 4.5% fat, 5.5% fiber by weight, and carbohydrates 63%, protein 24%, and fat 13% by caloric value. Mice were randomly allocated into the burn or sham groups, although we ensured subsequently that the starting weights of each group were not statistically different.

2.2 Brass plate assembly

Brass plates measuring 2×2×0.25, 1×1×0.25, or 1×2×0.25 cm were cut from brass plate stock (Small Parts, Amazon.com) then welded to metal screws. This assembly was then screwed into the ends of Teflon/PTFE round rods (www.smallparts.com) cut to size. This work was done in the machine shop at the University of Miami.

2.3 Burn injury

On the day of burn injury, anesthesia was induced using inhaled 1–3% isoflurane with supplemental oxygen and maintained with an intra-peritoneal injection of 100 mg/kg ketamine (Ketaset, Fort Dodge Animal Health, Fort Dodge, IA, USA) and 15 mg/kg xylazine (TranquiVed, Vedco, St. Joseph, MO, USA). After adequate sedation was achieved, the fur was removed by close shaving with clippers. Residual hair stubble was removed with the application of Nair© as per the manufacturer's instructions. Mice were then washed, dried, and weighed, and total body surface area was calculated according to the Meeh equation, BSA=k mass$^{0.667}$, where BSA is body surface area expressed in square centimeters and mass is expressed in grams, using the constant k=9.822 as we previously determined [19].

Mice were given a first dose of buprenorphine (s.c. 0.1 mg/kg in 0.1 cc, Buprenex, Rechitt Benchiser, Hull, England) to ensure effective analgesia upon wakening. The plate-rod contraption was immersed in a water bath (100°C) and blotted dry prior to use to avoid steam injury. Burn injuries were induced by balancing the brass plates/rods assembly on the dry dorsum with full skin contact, taking care to avoid the spine and upper and lower extremities. The dorsal surface was used rather than the ventral to avoid organ damage. Duration of contact was varied from 5 to 20 s but in the final model consisted of 5 s of contact. Uniform contact was confirmed by the resulting red coloration of the skin observed after removal of the plate. Additional burns were made with appropriate area brass plates in order to achieve the desired TBSA burn percentage.

Mice were resuscitated immediately following burn injury with a single intra-peritoneal injection of Lactated Ringer's, 2 cc/kg/% BSA burned. Trials of resuscitation with 4 cc/kg/% BSA and 6 cc/kg/% BSA were also performed. Buprenorphine (dosed as first) was administered every 12 h after burn for a total of six doses. Sham animals did not receive Nair© [because it induces a chemical burn and subsequent inflammation and muscle wasting, (unpublished data)] or burns but were given anesthesia, shaved, and provided fluid resuscitation and buprenorphine similar to the experimental group. Following burn injury, mice were housed individually with free access to food and drinking water and were weighed at the same time daily. Food and water intake were also measured daily in certain experiments by weighing the food and water bottle on day 1, then weighing the remaining food and water bottle the next day. Food and water consumed were calculated as the difference between starting and ending weights. Some mice persistently shredded the chow pellets, leaving noticeable quantities of crumbs on the cage floor. These rare mice (1–2 in 40) were excluded from the analysis.

2.4 Survival analysis

As much as possible, mice were not allowed to undergo spontaneous death because such death is not permitted as an endpoint according to the universities' standards for the humane and ethical treatment of research animals. If mice became moribund and displayed low to no motility, hunched posture, and declining body temperature, they were humanely euthanized and recorded as a death. Since most deaths occurred in first 48–72 h, mice were assessed at least every 12 h over the first 4 days.

2.5 Histology

Skin from the region of the burn injury, including unburned skin in the periphery, was excised and fixed in ice-cold neutral-buffered formalin. Skin from sham-treated mice was also taken for comparison. The skin was dehydrated, embedded in paraffin, and sectioned. Sections were de-waxed and stained with hematoxylin and eosin. Photographs were taken on an Olympus light microscope.

2.6 Necropsy and tissue analysis

Mice were euthanized at different time points (7, 14, 21, and 30 days) under general anesthesia with 1–3% isoflurane (inhaled) and supplemental oxygen followed by cardiac puncture and cervical dislocation. Platelet poor plasma was prepared from blood collected by cardiac puncture and placed on ice in EDTA microtainers, followed by centrifugation at 1,000×g for 15 min, removal of the plasma, and a second centrifugation at 10,000×g for 10 min at 4°C. Organs (liver, epididymal fat pad, spleen and heart) and

muscles (gastrocnemius, quadriceps, and tibialis) were dissected, weighed, and snap-frozen in liquid nitrogen as described previously [20]. Carcasses were stripped of pelt and organs and stored frozen at −80°C for later analysis. Lean and fat carcass mass, bone mineral density, and bone mineral content were subsequently determined on thawed, stripped carcasses using the Lunar PIXImus II (GE Medical Systems), a fast, dual X-ray densitometer optimized for mice and rats.

2.7 Cross-sectional area quantification and western blotting analysis

Tibialis muscles from 20% BSA burn and sham groups at 14 days were harvested, weighed, flash frozen in isopentane cooled in liquid nitrogen, and sectioned via cryostat. Sections were stained with hematoxylin and eosin. Photographs were taken with an Olympus© light microscope. Cross-sectional areas of 600 and 587 tibialis muscle fibers in the sham and burn groups, respectively, were quantified by an investigator blinded to the sample identities using NIH ImageJ. Analysis and graphing were performed with Prism 5.0 (GraphPad). For Murf-1 expression, whole quadricep lysates were subjected to western blotting analysis as described [21] using antibodies directed against Murf-1, SC-32920 (Santa Cruz Biotechnology, Santa Cruz, CA, USA) and AB57865 (Abcam, Cambridge, MA, USA) and GAPDH 5174 (Cell Signaling, Beverly, MA, USA).

2.8 Serum analyte profiling

All samples were stored at −80°C until tested (Rules Based Medicine, Austin, TX, USA). Platelet poor plasma samples were thawed at room temperature, vortexed, spun at 13,000×*g* for 5 min for clarification, and 150 μL was removed for multiple analyte profiling (MAP) antigen analysis into a master microtiter plate. Using automated pipetting, an aliquot of each sample was introduced into one of the capture microsphere multiplexes of the RodentMAP 2.0. These mixtures of sample and capture microspheres were thoroughly mixed and incubated at room temperature for 1 h. Multiplexed cocktails of biotinylated reporter antibodies for each multiplex were then added robotically and, after thorough mixing, were incubated for an additional hour at room temperature. Multiplexes were developed using an excess of streptavidin–phycoerythrin solution, which was thoroughly mixed into each multiplex and incubated for 1 h at room temperature. The volume of each multiplexed reaction was reduced by vacuum filtration and the volume increased by dilution into matrix buffer for analysis. Analysis was performed in a Luminex 100 instrument, and the resulting data stream was interpreted using proprietary data analysis software developed at Rules-Based Medicine and licensed to Qiagen Instruments. For each multiplex, both calibrators and controls were included on each microtiter plate. Eight-point calibrators were run in the first and last column of each plate, and three-level controls were included in duplicate. Testing results were determined first for the high, medium, and low controls for each multiplex to ensure proper assay performance. Unknown values for each of the analytes localized in a specific multiplex were determined using four- and five-parameter, weighted, and non-weighted curve fitting algorithms included in the data analysis package.

2.9 Statistical analysis

Data analysis was carried out using GraphPad Prism Version 5.0. The Kaplan–Meier method was used to evaluate overall survival and log-rank (Mantel–Cox) was used for comparisons between groups. Repeated measures two-way ANOVA was used for body weight comparisons. Two-way ANOVA with Bonferroni post-test was used to evaluate differences by treatment group and time point for endpoint studies. Student's unpaired *t* test was used to compare plasma analyte levels between burned and sham groups. Data are reported as mean±standard deviation. A P value of <0.05 was considered significant for all analysis.

3 Results

3.1 Effects of contact time, percentage burn and resuscitation on survival

We sought to characterize a model of reproducible burn-injury-associated weight loss without excessive mortality. C57BL/6J mice were chosen in order to provide a baseline characterization in a strain commonly used for generating and maintaining transgenic and knockout lines. Young adult (12–16 weeks old) male mice in the plateau phase of growth were used. This age range was selected to ensure that the burn-induced muscle wasting represented loss of muscle mass rather than growth inhibition as might be observed with younger mice. Males were used exclusively due to early indications of a sex difference in survival, with males exhibiting a reduced overall survival as compared to females (data not shown).

Mice were anesthetized, shaved, depilated, dried, and weighed. A burn of the required size was inflicted using a combination of brass plates of several sizes held in direct contact with the mouse skin in dorsal and lateral flank positions (Fig. 1a, b). In initial trials, the time of contact between the brass plate and the skin was varied, and the burned skin and underlying musculature were evaluated by histology (Fig. 2) and for survival (Fig. 3a). Hematoxylin and eosin staining of mouse skin collected 7 days after burn

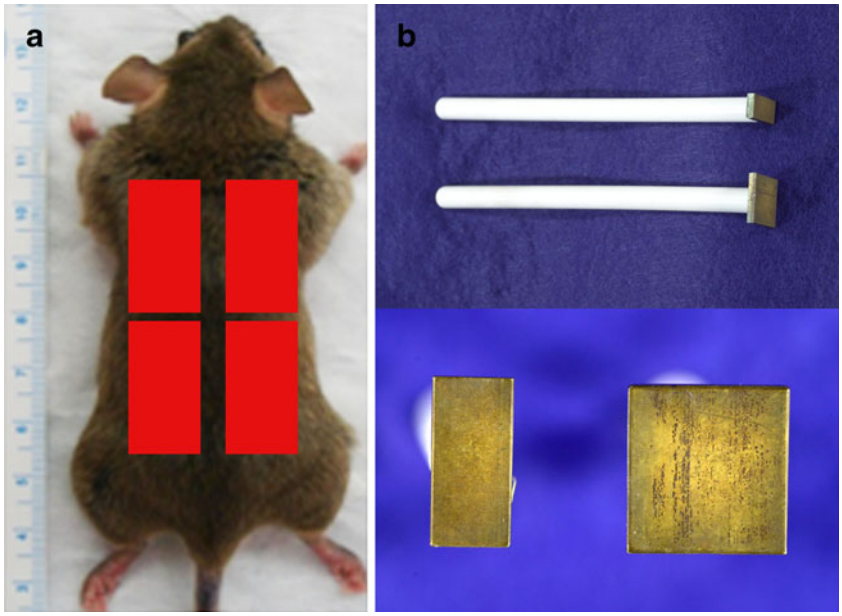

Fig. 1 Burn injury model. *Red boxes* indicate approximate are of plate placement on the dorsal aspect on either side of the vertebral column, avoiding the spine; however, lateral placement might also be necessary depending upon mouse total BSA and desired percent burn (**a**). Brass plates (1×2×0.25 and 2×2×0.25 cm) mounted on Teflon rods used for burn injury (**b**)

injury confirmed that full-thickness burns resulted from 5 s or greater of contact time. While in normal skin, the epidermis, dermis, hair follicle, sebaceous gland, and muscle are normal and intact, 5 s of contact resulted in necrosis of the epidermis, dermis, and dermal components without apparently affecting underlying muscle. In contrast, 10 or 15 s of contact time resulted in sloughing of the dermis, significant lymphocytic infiltrate and fracturing, fatty change, and necrosis of the skeletal muscle layer (Fig. 2). Because we were interested in systemic weight loss and muscle wasting rather than local muscle injury, 5 s of contact time was used in all subsequent experiments and in the final model.

Next, survival rates after burn injury in mice with differing contact time and percentage burn were determined (Fig. 3a). As in humans, murine survival following burn injury was directly related to percentage BSA burned. Contact times of

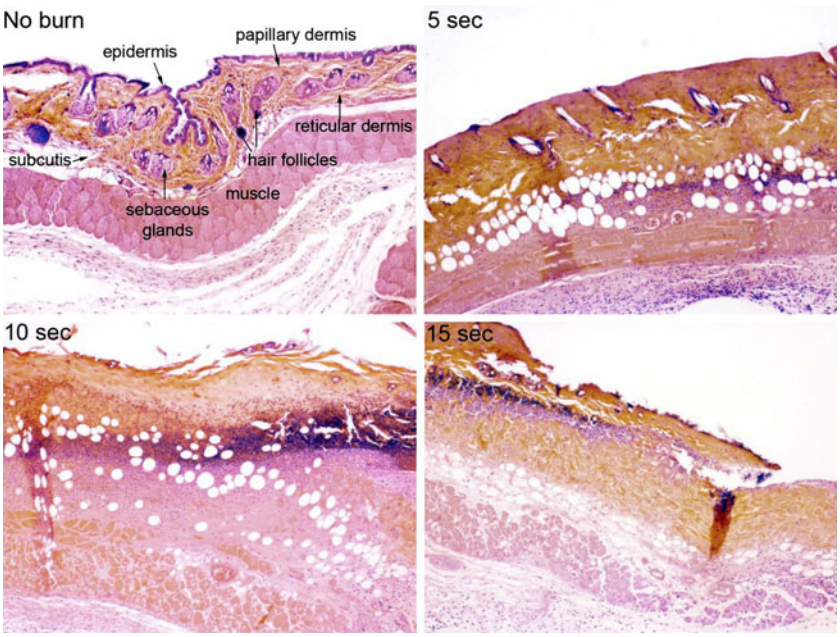

Fig. 2 Increased skin contact time with heated brass plates results in increased injury to the skin and underlying muscle. Hematoxylin and eosin staining of mouse skin 7 days after sham treatment (no burn) or after burn injury with the indicated contact time with heated brass plates. Normal skin (no burn) with epidermis, papillary and reticular dermis, hair follicles, sebaceous glands, subcutis, and muscle is labeled. Mouse skin subjected to 5 s of contact time exhibited loss of epidermis, nonviable dermis, with increased lymphocytic infiltration but absence of muscular involvement. With 10- and 15-s contact times, absence of the epidermis, sloughing of the dermis, and a significant lymphocytic infiltration are visible along with underlying muscle damage

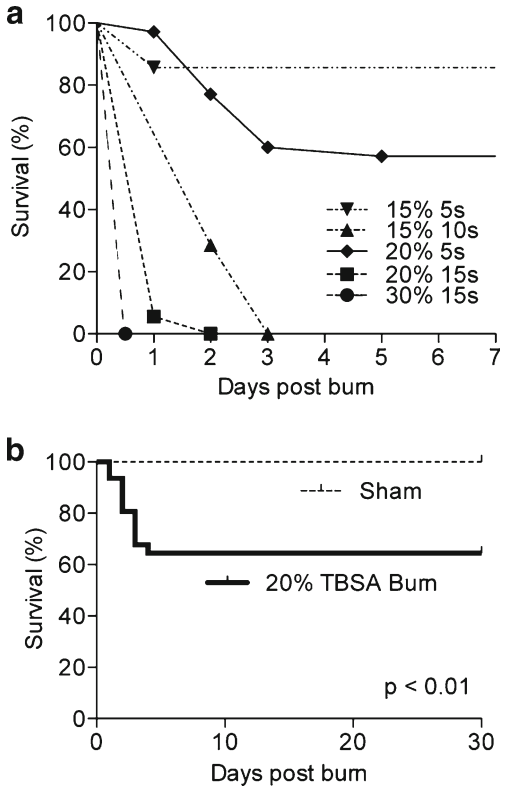

Fig. 3 Mortality is dependent upon % BSA burned and duration of skin-plate contact time. Kaplan–Meier curve shows reduced survival with increased percent body surface area (% BSA) burned and increased contact times (**a**). Thirty-day survival curve comparing sham to 20% BSA burn with 5 s contact time shows reduced overall survival (60%), with the majority of deaths occurring in the first 5–6 days following burn (**b**). Survival comparisons by log-rank (Mantel–Cox) test

10 s or longer resulted in 100% mortality, regardless of % BSA burned. With 5 s of contact time and 15% BSA burned, greater than 80% survival was observed. With 5 s of contact time and 20% BSA burned, greater than 50% survival was observed.

We next sought to evaluate the effect of fluid resuscitation on overall survival in the 5-s contact time and 20% BSA burn injury. Immediately after burn, animals were resuscitated with a single intra-peritoneal injection with 2 cc/kg/% BSA, 4 cc/kg/% BSA, and 6 cc/kg/% BSA of lactated ringers. In other studies, additional fluid was given 12 h after burn injury. No differences in gross behavior or overall survival were observed among groups (data not shown).

Based upon these results, a longer-term study of 5-s, 20% BSA burn, with 2 cc/kg/% BSA of lactated ringers resuscitation was undertaken. All mortalities in this model occurred in the first 5 days with no subsequent mortalities noted out to 30 days (n=48) (Fig. 3b).

3.2 Weight loss and muscle wasting

Weight loss was observed in both the 20% BSA burn and sham groups (Fig. 4a). Both groups demonstrate early weight loss, possibly due to reduced food intake as a result of buprenorphine treatment [in support of this, treatment of sham mice with buprenorphine resulted in an average 6.5% loss of body weight over 2 days versus carrier treated mice due to a ~40% reduction in food intake over the first day (unpublished data)]. While sham-treated mice regained the lost weight, burned mice did not; rather, they experienced an average 5% (range 5–15%) reduction in total body weight out to 30 days. The nadir for body weight in burned mice was 14 days, when total body mass was 92.6% of sham mice.

A time course analysis was performed to determine changes in body composition following burn injury. Mice were sacrificed at 7, 14, 21, and 30 days following burn injury or sham treatment and muscle and lean carcass mass were measured (Fig. 4b–e). The results indicated that the modest reduction in body weight in burned mice masked marked changes in body composition. Skeletal muscle mass was disproportionately reduced in animals receiving burns both by weight of individual muscle groups (Fig. 4b–d) as well as by Piximus analysis of the eviscerated, skinned carcass (Fig. 4e). The nadir of individual muscle masses appeared to be at 14 days. At this time, lean carcass mass had declined to 88.5%, while individual muscles were reduced to 70% (tibialis) of shams. Overall, lean carcass mass was most reduced at 7 days. Muscle and lean carcass loss persisted through the 30-day time point.

The tibialis muscle at 14 days was used to determine whether the reduction in muscle weight and LBM in burn mice was attributable to a reduction in overall muscle fiber cross-sectional area (Fig. 5). When compared to the sham mice, the burn mice exhibited a 30% reduction in tibialis muscle mass (P<0.001) and a 12% reduction in muscle fiber cross-sectional area (P<0.001) (Fig. 5b, c). Consistent with an overall reduction in fiber sizes, the distribution of muscle fiber cross-sectional areas was shifted leftward in the burn group (Fig. 5d). Consistent with prior reports of enhanced expression of the RNA for the skeletal muscle-specific ubiquitin ligase MuRF-1 [22], muscle wasting was associated with increased expression of proteins reacting MuRF-1-specific antibodies in western blotting analysis (Fig. 5e).

3.3 Weight, food, and water intake (0–80 days)

The sham group followed a normal growth curve after recovery of the initial weight loss due to buprenorphine administration. In contrast, the burn group exhibited a prolonged period of weight loss, with recovery of initial body weight at 35 days (Fig. 6a). At 80 days, the burn mice exhibited a 7% reduction in body weight compared to sham mice. Despite the reduced body weight, burned mice exhibited persistently increased water intake (90% greater than sham mice at 80 days), greatest at 4 days (156% greater

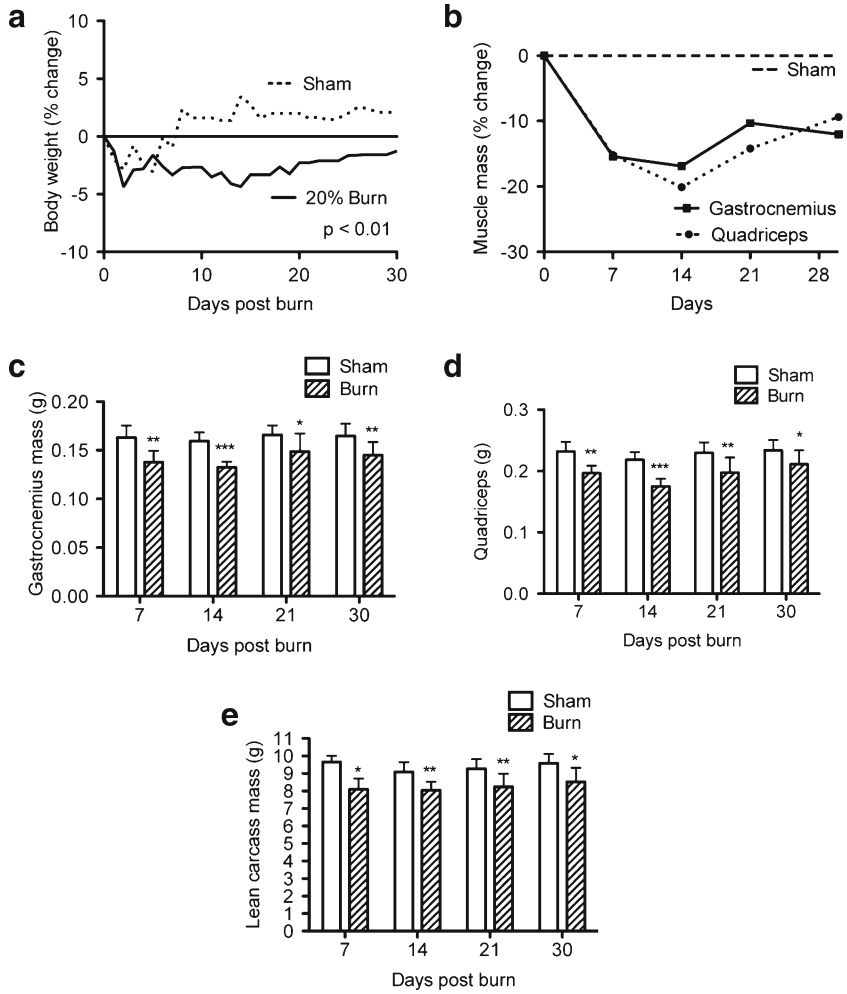

Fig. 4 Weight loss with disproportionate muscle loss in the 20% BSA burn model. Mice with 20% burn and 5-s contact time exhibited reduced overall body weight (**a**), with disproportionate reductions in quadriceps, gastrocnemius, and lean carcass mass (**b**–**e**). The nadir of lean body and muscle mass (quadriceps and gastrocnemius shown) occurred at 14 days. Starting weights were 7 days sham 28.26±1.2 g, 7 days burn 27.85±1.1 g, 14 days sham 25.77±2.1 g, 14 days burn 26.83±1.7 g, 21 days sham 27.96±0.8 g, 21 days burn 28.06±1.1 g, 30 days sham 27.04±2.0 g, 30 days burn 25.90±2.1 g, with no significant differences among groups. Results are mean±SD. N=6–27 per time point and group. ***P<0.001; **P<0.01; *P<0.05

than sham mice on day 4), and consuming overall twice as much water during the study period (Fig. 6b). The burn group also exhibited increased food intake for the duration of the study (44% greater than sham mice at 80 days), greatest at 14 days (188% greater than sham mice on day 14) (Fig. 6c), with overall consumption increased 74% over shams. The sham group showed generally stable food and water intake for the duration of 80 days, except on days 3–5 following buprenorphine administration (Fig. 6b, c).

3.4 Altered body composition

Changes in adipose tissue were more complex. Epididymal fat mass was significantly reduced from 14 through 30 days (Fig. 7a). However, carcass fat mass, reflecting adipose stores within muscle and cell membranes, was significantly reduced only at 14 days (Fig. 7b). Significant decreases in both bone mineral content (BMC) and bone mineral density (BMD) were also observed (Fig. 7c, d), with the greatest reductions at 14 days although reductions were trending toward significance at 30 days. At the nadir for total body weight of 14 days, fat mass had declined to 81.5% and bone mineral density was reduced to 92.5% of shams. Balancing the loss of muscle, fat and bone mass was hypertrophy of the abdominal organs. As in patients, absolute liver mass as well as liver to body mass ratios were increased after burn injury (Fig. 7e, f). At 14 days, burned mice showed significantly increased liver mass (117.5%) and liver to body mass ratios (123.2%) relative to sham controls. Liver hypertrophy did not resolve by 30 days. As well, spleen size was increased both in terms of actual mass and as a percentage of body weight through 30 days (Fig. 7g), while statistically significant hypertrophy of the heart was noted only at 14 and 21 days (Fig. 7h).

3.5 Serum profiling reveals acute phase response, increased cytokines, and chemokines

In patients, muscle wasting and hepatomegaly after burn have been linked to inflammation and heightened serum cytokine levels. To probe these parameters, we performed multiple analyte profiling on platelet poor plasma from burned and sham-treated mice at 14 days, the nadir for

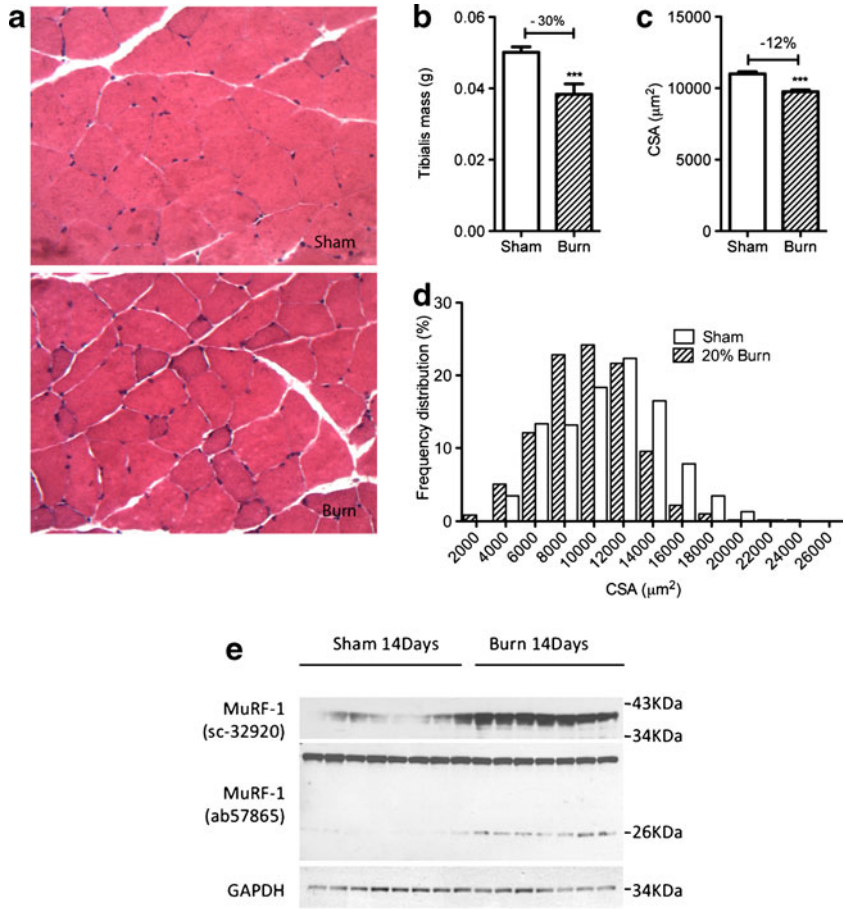

Fig. 5 Muscle fiber wasting at 14 days. Hematoxylin and eosin staining of tibialis anterior sections in sham and burned mice at 14 days (**a**). A 30% reduction in tibialis mass (mean weight±SD) was observed 14 days after 20% BSA burn injury ($P<0.001$) (**b**). Reduction in fiber cross-sectional area (CSA) in tibialis of burned mice ($N=587$ fibers from four mice) versus sham ($N=600$ fibers from three mice) at 14 days (**c**). A histogram shows the frequency distribution of muscle fiber CSA (**d**). Western blotting analysis of quadriceps lysate shows increased anti-MuRF-1 antibody immunoreactivity after burn injury (**e**). Starting weights were sham 31.21±2.6 and burn 32.74±1.25 g (N.S.). ***$P<0.001$

muscle weight, BMD and BMC, and the peak of hepatosplenomegaly (Fig. 6). Of 59 serum proteins tested, 54 were detectable above background. Of those, 23 demonstrated statistically significant (defined as $P<0.05$) variance between the burn group versus the sham group, 19 of which revealed differences that were greater than 1.5-fold or less than 0.75-fold sham levels, chosen as the criteria for potential biological significance.

In this analysis, the burned mice showed evidence of an acute phase response. The serum acute phase response proteins haptoglobin (3.66-fold), fibrinogen (2.82-fold), serum amyloid P (SAP) (2.39-fold), and C-reactive protein (1.96-fold) were all elevated. Consistent with these results, the major activator of the acute phase response, interleukin-6 (IL-6) [23, 24] was greatly elevated in burned mice (32±15 pg/mL) versus sham-treated mice, all of which had undetectable IL-6 levels. Other cytokines that were increased were CD40 ligand (1.73-fold) and oncostatin M (1.62-fold).

Chemokine levels also differed in burned mice at 14 days. Macrophage inflammatory protein (MIP)-2 (12.94-fold), KC-GROalpha (10.21-fold), monocyte chemoattractant protein (MCP)-5 (2.86-fold), MCP-3 (2.74-fold), MCP-1 (2.36-fold), RANTES (2.31-fold), and MIP-1 gamma (1.78-fold) were all increased. Of the growth factors measured, only vascular endothelial cell growth factor was significantly changed in burned mice to 1.53-fold. Of the other analytes tested, only tissue inhibitor of metalloproteinase-1 (4.19-fold), von Willebrand factor (3.05-fold), and myeloperoxidase (3.31) met the definition of significantly changed.

4 Discussion

In 1942, Cuthbertson first described the metabolic derangements in post-traumatic patients occurring in two phases, the "ebb" phase resulted in an initial reduction in metabolism which was followed by the "flow" phase, occurring 3–5 days later and characterized by a hypermetabolic state that, if left untreated, could lead to a physiologic exhaustion and death [25, 26]. Such derangements in metabolism and body composition including muscle and bone loss as well as organomegaly after burn injury remain a significant cause of long-term morbidity and mortality for patients [5, 26]. Understanding the signaling pathways governing these processes should lead to therapeutic interventions that improve survival and quality of life. Herein we describe a mouse model of burn injury that reproduces the chronic human pathophysiological

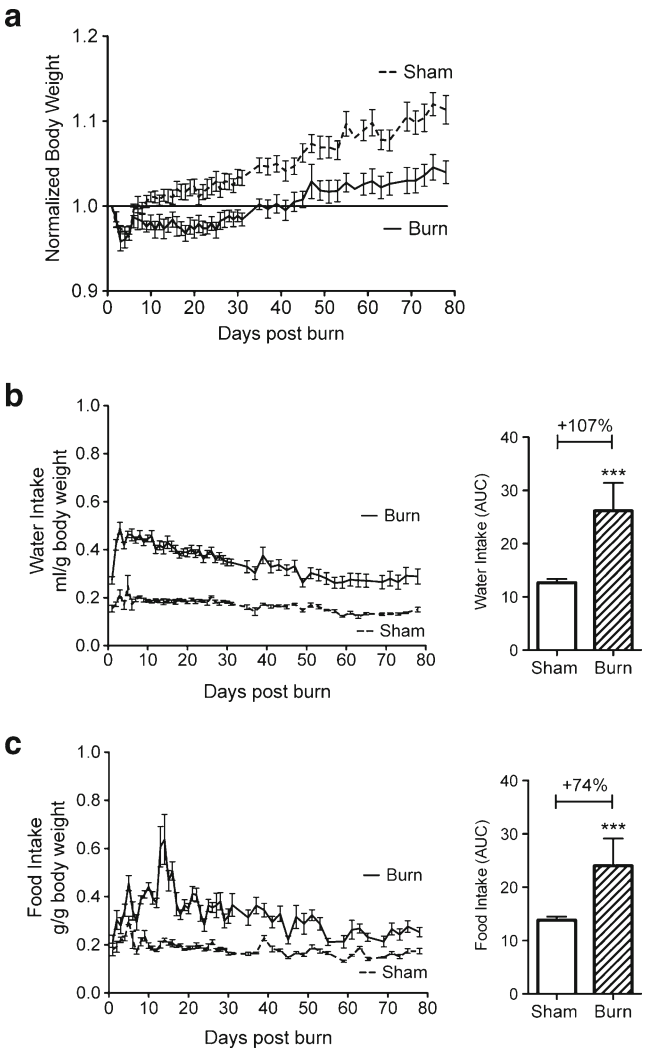

Fig. 6 Twenty percent BSA burn leads to a prolonged reduction in body weight despite chronic hyperphagia and polydipsia. Mice with burn injury experienced significantly reduced body weight. Recovery of starting body weight occurred at 35 days, but weight remained reduced versus shams out to 80 days when the experiment was terminated (**a**). Both daily water (**b**) and food (**c**) intake (mean±SD) were significantly increased following 20% burn injury out to 80 days. Total intake calculated as the area under the curve (*AUC*) for each mouse was also increased (*bar graphs*). The mice in the burn group were slightly larger at day 0, sham 25.67±0.3 g (N=8) and burn 27.76±0.4 (N=14) (p<0.01)

response following severe burn. This description of chronic peripheral wasting and organ hypertrophy in C57BL/6J mice provides a baseline for future pharmacological and genetic approaches to dissecting the molecular mechanisms underlying burn-injury-associated cachexia.

Similar to clinical observations, the mouse exhibits increased mortality with increasing percent BSA burned [7]. Furthermore, we observed that as contact time increased, mortality increased precipitously (Fig. 3). Survival data taken together with the histological data suggest that the length of contact time is directly related to the depth of injury locally and the magnitude of the response systemically. Ultimately we settled upon 5 s of contact time to burn 20% of the BSA and analyzed the mice out to 30 days.

This approach resulted in a 60% survival rate and modest reductions in total body mass that mask a disproportionately large loss of muscle and lean body mass, with a concomitant reduction in muscle fiber cross sectional area (Figs. 4 and 5). Loss of bone mineral content, bone mineral density, and fat was also observed as in human burn patients [4] (Fig. 7). Organomegaly after burn injury contributes to increased total body weight, helping to mask the severity of wasting. Similar to human subjects, liver hypertrophy was noted, and moreover, increased weight of the gut and lungs was also observed (data not shown) [13, 14, 26] (Fig. 7). The results mimic changes observed in burn patients and reflect a shift of amino acid and fat stores away from peripheral compartments toward visceral compartments, ostensibly a pro-survival mechanism to preserve abdominal organ function, provide substrates for wound healing, and to promote the immune response.

The burned mice also exhibited a profound and prolonged period of increased food and water intake up to 80 days which is consistent with the increased nutritional requirements observed in severe burn patients who remain hypermetabolic with increased resting energy expenditure for up to 2 years following burn injury [4, 26] (Fig. 6). It has been shown repeatedly that a lack of increased nutritional support during this period reduces overall survival and recovery in severe burn patients [27]. Also, the mice exhibited a prolonged period of significant polydipsia out to 80 days, likely attributable acutely to the water and heat loss commonly found following burn (water loss can approach 4,000 mL/m^2 burn area per day) and chronically due to a persistent hypermetabolic state [26].

In addition to the pathophysiological changes and temporal similarities, we also observe systemic inflammation as in convalescent human burn patients. As reported in prior studies in mice and humans with burn injury, coincident with skeletal muscle and fat wasting and organ hypertrophy, we observed an increase in levels of the cytokines, as well as clear evidence of a chronic acute phase response, as represented by elevations in haptoglobin, fibrinogen, SAP, and CRP [11, 14, 28] (Fig. 8). Such chronic inflammation is a common observation across experimental and clinical cachexia and is likely a root cause of the reduced body mass, muscle and fat wasting, and organomegaly observed after burn injury. Specifically IL-6 is significantly elevated in burn patients and has been demonstrated to be a predictor of outcomes in severely burned patients [26, 28]. In support of this theory, systemic IL-6 treatment alone, in the absence of other injury or treatment, promotes loss of total body weight, muscle mass, and fat mass, along with profound hepatosplenomegaly and increased gut, kidney, and lung mass [24, 29]. Which effects

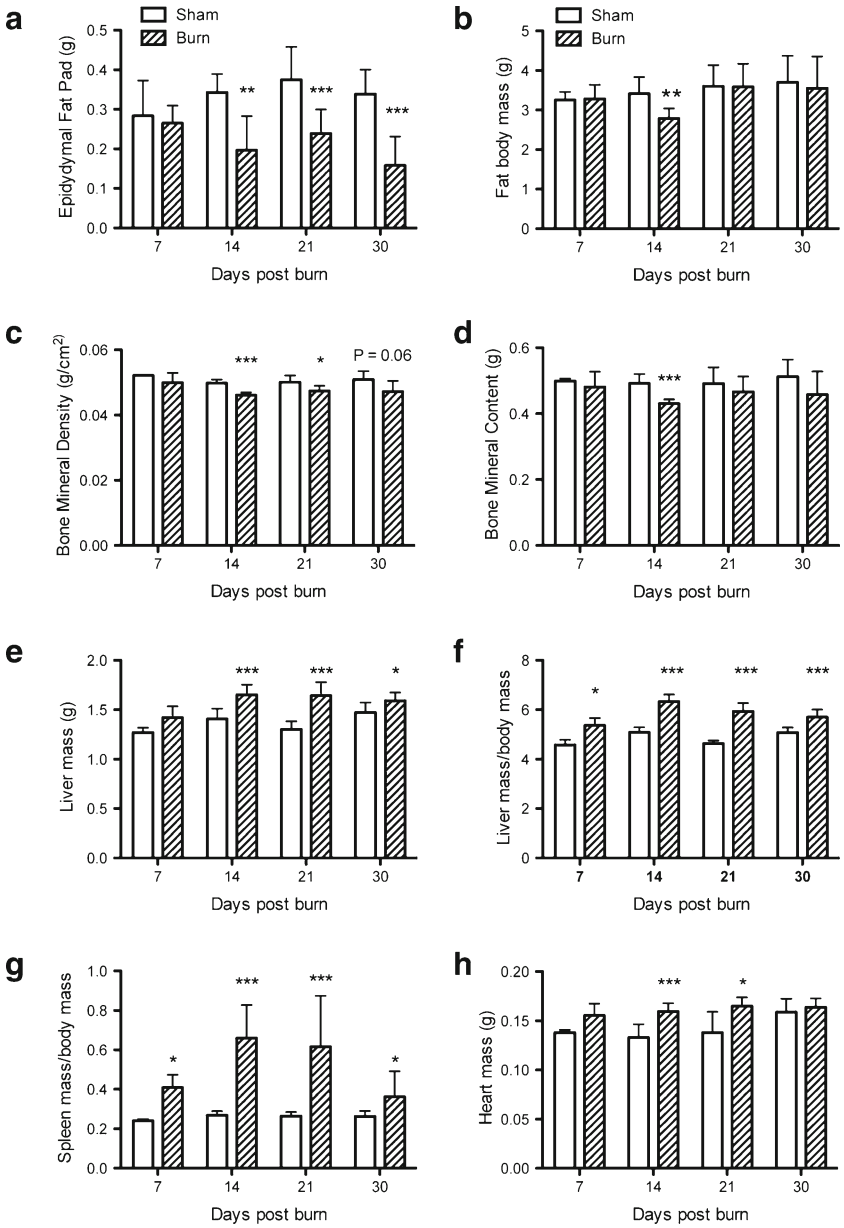

Fig. 7 Fat and bone loss with hepatosplenomegaly and cardiac hypertrophy following 20% BSA burn. Epididymal fat pad in 20% BSA burn is significantly reduced starting with day 14 and continuing through 30 days (**a**). Total body fat content by Piximus was significantly reduced at 14 days (**b**). Bone mineral density (*BMD*) and bone mineral content (*BMC*) by Piximus were significantly reduced at 14 days (**c**–**d**). The nadir for fat (epididymal, body fat mass), BMD, and BMC occurred at 14 days, with concomitant peak liver size (**e**–**f**). Spleen and heart mass were also elevated after burn (**g**–**h**). Results are mean± SD. Starting weights are as in Fig. 4. N=6–27 per time point and group. ***P<0.001; **P<0.01; *P<0.05

on body composition are the direct effect of IL-6 signaling and which are indirect is not altogether clear. In the case of IL-6 treatment, however, the increase in liver mass was due to both hepatocyte hypertrophy (necessary for the massively increased protein synthetic requirements for the acute phase response) as well as hyperplasia, while the increase in gut mass was due to inhibition of enterocyte apoptosis [30–34]. IL-6 may also play a role in promoting muscle catabolism directly in burn injury, as in other models of muscle wasting [21].

Importantly, we also observe the long-term nature of chronic body changes, inflammation, and nutritional requirements measured in burn patients [4, 11] (Table 1). The best approximations of rat age to human years indicate that during the adult phase of life, 11.8 rat days is equivalent to 1 human year [35]. Given that laboratory mice have similar developmental and physiological benchmarks, the 2 to 4 weeks of muscle wasting we observe in mice would be similar to wasting of 1.2 to 2.5 years duration in burn patients [3, 4, 11].

While many investigators use murine models of burn injury, a single, complete description of post-burn cachexia in the mouse was lacking in the literature. We sought to report our experience and characterization to facilitate others' adoption of the model for anti-cachexia research. There are several limitations to our study. One discrepancy between our mouse model and human findings is our reduced overall survival (60%) as compared to human 20% TBSA burn subjects who historically exhibit survival of >90% [2]. Of course, our mice are untreated, save initial anesthesia and fluid resuscitation,

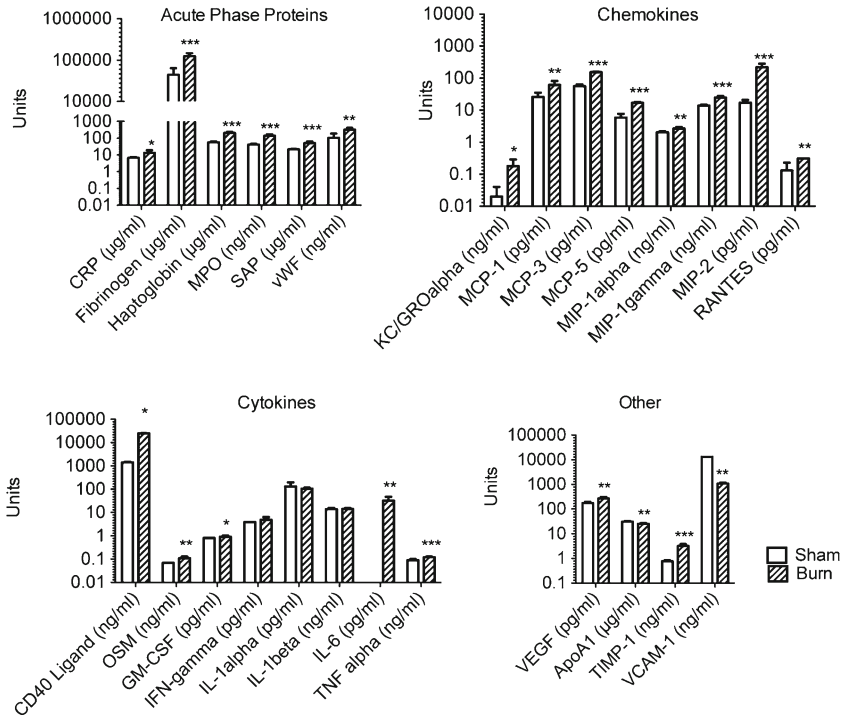

Fig. 8 Twenty percent BSA burn injury leads to increases in plasma acute phase proteins, chemokines, and cytokines. Multiple analyte profiling was performed on platelet-poor plasma in sham and 20% BSA burn mice at 14 days. Results are mean±SD, ***$P<0.001$; **$P<0.01$; *$P<0.05$

Table 1 Twenty percent TBSA burn in mice reproduces pathophysiological changes observed in human burn injury

	Human	Mouse
Burn size	53%	20%
3rd degree burn size	43%	20%
Length of hospital stay	31 days	14 days
Body weight change	−2%	−5%
LBM	−4.1%	−11.5%
FBM	+3%	−19%
BMC	−3%	−12.4%
BMD	−2%	−7.4%
Liver mass	+80–120%	+34–50%
Sepsis rate	25%	N.D.
Evidence of inflammation		
Cytokines	Elevated	Elevated
Chemokines	Elevated	Elevated
Acute phase reactants	Elevated	Elevated
Evidence of hypermetabolism	Increased REE	Hyperphagic but weight stable
Caloric intake	1,500 kcal/m^2 BSA +1,500 kcal/m^2 burn	~6,000 kcal/m^2
	1.25-fold RDI	3-fold normal
Duration of hypermetabolism	Up to 2 years	At least 80 days
Duration of wasting	Up to 2 years	At least 80 days

Pathophysiologic changes in mice with 20% TBSA burn at 14 days as compared to those found in human burn subjects (11)

LBM lean body mass, *FBM* fat body mass, *BMC* bone mineral content, *BMD* bone mineral density

while patients with severe burn are intensively treated. Our observed mortality is similar to that reported by some groups using 25% BSA scald models [36]. Greater mortality than others might be due to a combination of greater contact in this study due to depilation and use of brass plates, differences in calculating BSA, and conventional versus barrier housing; however, as in patients, lethality and the presence of long-term wasting were well correlated. Lower percentage burns caused no deaths and no total body weight loss. We chose the %BSA that resulted in a major physiological challenge, sometimes resulted in death and always resulted in long-term consequences for survivors. We chose to use contact burn injury using plates of specific dimensions rather than scald due to the greater control of percentage TBSA burned. Scald models generally use a single mold that does not permit varying the burn size. In contrast, our approach permits precise application of burn injury across age and weight ranges or for mice of altered body shape and composition, including obese, hypermuscular, or otherwise size-altered animals.

Cachexia is a devastating syndrome affecting trauma, surgical, and critically or chronically ill patients, including burn. However, the severity and chronicity of cachexia in burn patients is unique. Several clinical studies have led to therapeutic advancements for the treatment of the hypercatabolic state in the acute period following burn resulting in improvements in the degree of cachexia chronically. These therapies include propranolol [37], testosterone, oxandrolone [38], recombinant human growth hormone, insulin-like growth factor [39, 40], and growth hormone [26, 41] with favorable outcomes. The exact mechanisms behind the efficacy of these interventions, particularly

propanolol and anabolic steroids, are largely unknown and need to be further studied. The baseline data we present on long-term changes after burn injury in the C57BL/6J mouse can provide a baseline for future studies of burn-injury-associated cachexia in evaluating the efficacy of therapeutic or molecular interventions and in genetically modified mice.

Acknowledgments The authors thank Billy Olafson for assistance with animal experiments and Wayne Balkan, Ph.D., for assistance with the Piximus imaging system. This work was supported in part by the Burn Center at Jackson Memorial Hospital and the University of Miami and by grants to T.A.Z from the National Cancer Institute CA122596, from the National Institute for General Medical Studies GM092758, and from the American Cancer Society. Additional support was provided by an administrative supplement to promote diversity in health related research to F.E.P. GM092758-01A1S1. The authors of this manuscript certify that they comply with the ethical guidelines for authorship and publishing in the Journal of Cachexia, Sarcopenia and Muscle [42].

Conflict of interest The authors declare they have no conflicts of interest.

References

1. ABA. Burn incidence and treatment in the US: 2011 fact sheet. Chicago: American Burn Association; 2011. Accessed 23 Aug 2011.
2. ABA. American Burn Association, National Burn Repository. Chicago: American Burn Association; 2009.
3. Pereira C, Murphy K, Jeschke M, Herndon DN. Post burn muscle wasting and the effects of treatments. Int J Biochem Cell Biol. 2005;37:1948–61.
4. Jeschke MG, Gauglitz GG, Kulp GA, Finnerty CC, Williams FN, Kraft R, et al. Long-term persistence of the pathophysiologic response to severe burn injury. PLoS One. 2011;6:e21245.
5. Hart DW, Wolf SE, Mlcak R, Chinkes DL, Ramzy PI, Obeng MK, et al. Persistence of muscle catabolism after severe burn. Surgery. 2000;128:312–9.
6. Pearson E, Soroff HS, Reiss E. Metabolic derangements in burns. J Am Diet Assoc. 1956;32:223–8.
7. Jeschke MG, Mlcak RP, Finnerty CC, Norbury WB, Gauglitz GG, Kulp GA, et al. Burn size determines the inflammatory and hypermetabolic response. Crit Care. 2007;11:R90.
8. Tan BH, Fearon KC. Cachexia: prevalence and impact in medicine. Curr Opin Clin Nutr Metab Care. 2008;11:400–7.
9. Morley JE, Thomas DR, Wilson MM. Cachexia: pathophysiology and clinical relevance. Am J Clin Nutr. 2006;83:735–43.
10. Borsheim E, Chinkes DL, McEntire SJ, Rodriguez NR, Herndon DN, Suman OE. Whole body protein kinetics measured with a non-invasive method in severely burned children. Burns. 2010;36:1006–12.
11. Jeschke MG, Chinkes DL, Finnerty CC, Kulp G, Suman OE, Norbury WB, et al. Pathophysiologic response to severe burn injury. Ann Surg. 2008;248:387–401.
12. Strock LL, Singh H, Abdullah A, Miller JA, Herndon DN. The effect of insulin-like growth factor I on postburn hypermetabolism. Surgery. 1990;108:161–4.
13. Barrow RE, Hawkins HK, Aarsland A, Cox R, Rosenblatt J, Barrow LN, et al. Identification of factors contributing to hepatomegaly in severely burned children. Shock. 2005;24:523–8.
14. Jeschke MG, Micak RP, Finnerty CC, Herndon DN. Changes in liver function and size after a severe thermal injury. Shock. 2007;28:172–7.
15. Tomera JF, Lilford K. Co-modulation between acetylcholinesterase and cyclic nucleotide signal transduction systems in burn trauma. Methods Find Exp Clin Pharmacol. 1995;17:89–105.
16. Madihally SV, Toner M, Yarmush ML, Mitchell RN. Interferon gamma modulates trauma-induced muscle wasting and immune dysfunction. Ann Surg. 2002;236:649–57.
17. Tan Y, Peng X, Wang F, You Z, Dong Y, Wang S. Effects of tumor necrosis factor-alpha on the 26S proteasome and 19S regulator in skeletal muscle of severely scalded mice. J Burn Care Res. 2006;27:226–33.
18. Tzika AA, Astrakas LG, Cao H, Mintzopoulos D, Zhang Q, Padfield K, et al. Murine intramyocellular lipids quantified by NMR act as metabolic biomarkers in burn trauma. Int J Mol Med. 2008;21:825–32.
19. Cheung MC, Spalding PB, Gutierrez JC, Balkan W, Namias N, Koniaris LG, et al. Body surface area prediction in normal, hypermuscular, and obese mice. J Surg Res. 2009;153:326–31.
20. Zimmers TA, Davies MV, Koniaris LG, Haynes P, Esquela AF, Tomkinson KN, et al. Induction of cachexia in mice by systemically administered myostatin. Science. 2002;296:1486–8.
21. Bonetto A, Aydogdu T, Kunzevitzky N, Guttridge DC, Khuri S, Koniaris LG, et al. STAT3 activation in skeletal muscle links muscle wasting and the acute phase response in cancer cachexia. PLoS One. 2011;6:e22538.
22. Lang CH, Huber D, Frost RA. Burn-induced increase in atrogin-1 and MuRF-1 in skeletal muscle is glucocorticoid independent but downregulated by IGF-I. Am J Physiol Regul Integr Comp Physiol. 2007;292:R328–36.
23. Fattori E, Cappelletti M, Costa P, Sellitto C, Cantoni L, Carelli M, et al. Defective inflammatory response in interleukin 6-deficient mice. J Exp Med. 1994;180:1243–50.
24. Strassmann G, Fong M, Windsor S, Neta R. The role of interleukin-6 in lipopolysaccharide-induced weight loss, hypoglycemia and fibrinogen production, in vivo. Cytokine. 1993;5:285–90.
25. Cuthbertson DP, Angeles Valero Zanuy MA, Leon Sanz ML. Post-shock metabolic response. 1942. Nutr Hosp. 2001;16:176–82. discussion 5–6.
26. Williams FN, Jeschke MG, Chinkes DL, Suman OE, Branski LK, Herndon DN. Modulation of the hypermetabolic response to trauma: temperature, nutrition, and drugs. J Am Coll Surg. 2009;208:489–502.
27. Mosier MJ, Pham TN, Klein MB, Gibran NS, Arnoldo BD, Gamelli RL, et al. Early enteral nutrition in burns: compliance with guidelines and associated outcomes in a multicenter study. J Burn Care Res. 2011;32:104–9.
28. Padfield KE, Zhang Q, Gopalan S, Tzika AA, Mindrinos MN, Tompkins RG, et al. Local and distant burn injury alter immune-inflammatory gene expression in skeletal muscle. J Trauma. 2006;61:280–92.
29. Black K, Garrett IR, Mundy GR. Chinese hamster ovarian cells transfected with the murine interleukin-6 gene cause hypercalcemia as well as cachexia, leukocytosis and thrombocytosis in tumor-bearing nude mice. Endocrinology. 1991;128:2657–9.
30. Jin X, Zhang Z, Beer-Stolz D, Zimmers TA, Koniaris LG. Interleukin-6 inhibits oxidative injury and necrosis after extreme liver resection. Hepatology. 2007;46:802–12.

31. Zimmers TA, McKillop IH, Pierce RH, Yoo JY, Koniaris LG. Massive liver growth in mice induced by systemic interleukin 6 administration. Hepatology. 2003;38:326–34.
32. Jin X, Zimmers TA, Perez EA, Pierce RH, Zhang Z, Koniaris LG. Paradoxical effects of short- and long-term interleukin-6 exposure on liver injury and repair. Hepatology. 2006;43:474–84.
33. Zimmers TA, Pierce RH, McKillop IH, Koniaris LG. Resolving the role of IL-6 in liver regeneration. Hepatology. 2003;38:1590–1. author reply 1.
34. Jin X, Zimmers TA, Zhang Z, Peirce RH, Koniaris LG. Interleukin-6 is an important in vivo inhibitor of intestinal epithelial cell death in mice. Gut. 2009.
35. Quinn R. Comparing rat's to human's age: how old is my rat in people years? Nutrition. 2005;21:775–7.
36. Gelfand JA, Donelan M, Hawiger A, Burke JF. Alternative complement pathway activation increases mortality in a model of burn injury in mice. J Clin Invest. 1982;70:1170–6.
37. Gauglitz GG, Williams FN, Herndon DN, Jeschke MG. Burns: where are we standing with propranolol, oxandrolone, recombinant human growth hormone, and the new incretin analogs? Curr Opin Clin Nutr Metab Care. 2011;14:176–81.
38. Miller JT, Btaiche IF. Oxandrolone treatment in adults with severe thermal injury. Pharmacotherapy. 2009;29:213–26.
39. Jeschke MG, Herndon DN, Barrow RE. Insulin-like growth factor I in combination with insulin-like growth factor binding protein 3 affects the hepatic acute phase response and hepatic morphology in thermally injured rats. Ann Surg. 2000;231:408–16.
40. Heszele MF, Price SR. Insulin-like growth factor I: the yin and yang of muscle atrophy. Endocrinology. 2004;145:4803–5.
41. Branski LK, Herndon DN, Barrow RE, Kulp GA, Klein GL, Suman OE, et al. Randomized controlled trial to determine the efficacy of long-term growth hormone treatment in severely burned children. Ann Surg. 2009;250:514–23.
42. von Haehling S, Morley JE, Coats AJ, Anker SD. Ethical guidelines for authorship and publishing in the Journal of Cachexia, Sarcopenia and Muscle. J Cachex Sarcopenia Muscle. 2010;1:7–8.